

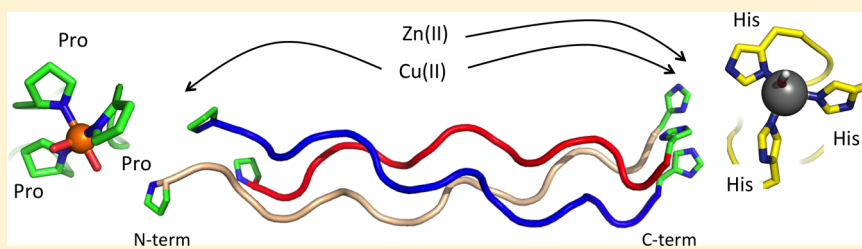
## Metal Stabilization of Collagen and de Novo Designed Mimetic Peptides

Avanish S. Parmar,<sup>†,‡</sup> Fei Xu,<sup>‡</sup> Douglas H. Pike,<sup>‡</sup> Sandeep V. Belure,<sup>‡</sup> Nida F. Hasan,<sup>‡</sup> Kathryn E. Drzewiecki,<sup>§</sup> David I. Shreiber,<sup>§</sup> and Vikas Nanda<sup>\*‡</sup>

<sup>†</sup>Department of Biotechnology & Bioinformatics, School of Life Sciences, University of Hyderabad, Gachibowli, Hyderabad-500046, Telangana, India

<sup>‡</sup>Center for Advanced Biotechnology and Medicine, Department of Biochemistry and Molecular Biology Robert Wood Johnson Medical School and <sup>§</sup>Department of Biomedical Engineering, Rutgers, The State University of New Jersey, Piscataway, New Jersey 08854, United States

### Supporting Information



**ABSTRACT:** We explore the design of metal binding sites to modulate triple-helix stability of collagen and collagen-mimetic peptides. Globular proteins commonly utilize metals to connect tertiary structural elements that are well separated in sequence, constraining structure and enhancing stability. It is more challenging to engineer structural metals into fibrous protein scaffolds, which lack the extensive tertiary contacts seen in globular proteins. In the collagen triple helix, the structural adjacency of the carboxy-termini of the three chains makes this region an attractive target for introducing metal binding sites. We engineered His<sub>3</sub> sites based on structural modeling constraints into a series of designed homotrimeric and heterotrimeric peptides, assessing the capacity of metal binding to improve stability and in the case of heterotrimers, affect specificity of assembly. Notable enhancements in stability for both homo- and heteromeric systems were observed upon addition of zinc(II) and several other metal ions only when all three histidine ligands were present. Metal binding affinities were consistent with the expected Irving–Williams series for imidazole. Unlike other metals tested, copper(II) also bound to peptides lacking histidine ligands. Acetylation of the peptide N-termini prevented copper binding, indicating proline backbone amide metal-coordination at this site. Copper similarly stabilized animal extracted Type I collagen in a metal-specific fashion, highlighting the potential importance of metal homeostasis within the extracellular matrix.

**D**e novo design of metal–protein complexes has advanced our understanding of metal control on structure and function.<sup>1–3</sup> Engineered structural metals have been successfully used to enforce the folding and oligomerization of proteins.<sup>4–9</sup> Most work in this area has focused on globular proteins, while interactions of metals with fibrous proteins such as collagen remain poorly understood. This is despite the fact that collagens are the most abundant proteins by mass in animals, playing important functional roles in many biological processes. The fibrillar structure of collagen provides tensile strength and flexibility to tissue, cartilage, and bone. The interaction of metals with collagen is also of industrial interest. Metals such as chromium and aluminum are used as tanning agents and change both the color and structure of leather through specific interactions with collagen.<sup>10–12</sup>

Collagen has a unique three-dimensional structure, composed of three chains that oligomerize into the triple-helix fold. Individual chains are in a polyproline II conformation, which

supercoil in the triple helix. In natural collagens, the fibrillar region extends over a thousand amino acids and contains post-translational modifications, making it challenging to express, purify, and characterize its biochemical and biophysical behavior. As such, short collagen mimetic peptide (CMPs) systems have been essential tools in exploring the molecular basis for stability, specificity, and higher order assembly. The most stable CMPs using biogenic amino acids consist of repeating (Gly-Pro-Hyp)<sub>n</sub> triplets.<sup>13</sup> CMPs have been designed to probe the role of amino acid sequence on folding kinetics,<sup>14</sup> stability of the triple-helix,<sup>15–23</sup> and triple-helical geometry.<sup>15,24</sup>

The introduction of novel metal sites into proteins provides a way to enhance stability and use metal binding as a structural switch. There are several approaches to structure-guided design

**Received:** May 6, 2015

**Revised:** July 30, 2015

**Published:** July 30, 2015



of metalloproteins. One is to construct protein folds that accommodate a metal by parameterizing backbone geometry and key ligand contacts around a metal—a de novo approach.<sup>25</sup> Alternatively, a metal binding site can be designed into a known fold.<sup>5</sup> In this study, we explore whether the latter approach can be used to introduce structural metals into the collagen fold in order to confer stability and specificity of triple-helix folding. Unlike globular proteins, collagen has an extended structure and a limited number of tertiary contacts, making it challenging to engineer a metal binding site. However, the structural adjacency of the three chain termini of the triple-helix makes those sites potentially suited for this purpose.

Connecting the chain termini in CMPs through side chain-backbone linkages<sup>26–30</sup> or other templates<sup>31</sup> at chain termini was shown to drive folding and enhance the stability of short Gly-Xxx-Yyy repeats, facilitating host–guest studies of amino acid substitutions in the triple-helix. Similarly, the inclusion of metal chelating ligands such as bipyridine,<sup>32–34</sup> catechol,<sup>35</sup> and imidazole<sup>36</sup> at the ends of chains increased stability of the triple helix. Metal-binding sites introduced at the ends of CMPs have been utilized to promoted higher order assembly of collagen nanostructures.<sup>34,36–41</sup> Here, we examine whether the inclusion of metal coordinating biogenic amino acids can enhance model peptide stability and specificity of assembly.

We are also interested in whether metal binding can be used as a tool to probe or enhance the specificity of oligomeric interactions between the three chains in the collagen triple-helix. A majority of studies of synthetic CMP systems have focused on homotrimers where the three chains have the same sequence. However, some naturally occurring collagens exist as heterotrimers; for example, Type I collagen consists of both an  $\alpha_1$  and  $\alpha_2$  gene product which assemble as an  $\alpha_1:\alpha_1:\alpha_2$  complex. *abc*-type heterotrimers are also possible, as in the case of Type V collagen which can exist as an  $\alpha_1:\alpha_2:\alpha_3$  complex. Therefore, there is significant interest in developing CMP systems that form specific heterotrimers, providing model systems to study biophysical effects of disease causing mutations in a heteromeric context.<sup>42,43</sup> A number of molecular strategies have been used, including the introduction of disulfide bridges,<sup>44–46</sup> and exploiting complementary pairing of electrostatic interactions.<sup>47–49</sup> Analysis of natural collagen sequences shows an unusually high frequency of charged amino acids that participate in favorable interchain interactions.<sup>50–52</sup> Brodsky and co-workers have shown these interactions increase thermal stability in CMPs.<sup>53–55</sup> Heterotrimers incorporating extensive charge-pair networks have also been designed using automated computational approaches.<sup>56–58</sup>

We use metal-assisted assembly of CMPs to examine whether metal binding can modulate stability and specificity of heterotrimer assembly. C-Terminal histidines are introduced into a previously designed *abc*-type CMP heterotrimer.<sup>56</sup> Heterospecific assembly allows us to control histidine ligand stoichiometry and study its effect on metal affinity. In the triple helix, the three chains interact in a staggered fashion with a one-residue shift in register between adjacent chains. We sought to determine whether varying linker lengths that connect histidine ligands to the triple helix could produce structurally constrained designs that would only show an enhancement in stability in the right relative register of the three chains. Although stability enhancements were clearly observed in nearly all peptide systems, metal binding sites as designed were unable to discriminate the correct register of the *abc*-type CMPs, indicating that structural flexibility of the binding site was a

confounding factor. In the course of studying this system, a secondary histidine-independent copper(II) binding mode was found in the CMPs and in animal-extracted Type I collagen. This work highlights the challenges in structure-guided design of metal binding sites into a triple-helical scaffold.

## EXPERIMENTAL PROCEDURES

**Peptide Synthesis and Sequences.** The peptides were synthesized using solid-phase Fmoc chemistry at the Tufts University Core Facility, Boston, MA. Unless otherwise specified, N- and C-termini were uncapped. Peptides were purified to 95% purity by reverse-phase high-performance liquid chromatography (HPLC), and products were verified by mass spectrometry (Figure S9). The sequences of the characterized peptides are listed below:

(i) (POG)<sub>n</sub> and (PPG)<sub>n</sub> domain peptides

(POG) <sub>n</sub> PAH	POGPOGPOGPOGPOGPOGPOG <b>PAH</b>
(POG) <sub>n</sub> AH	POGPOGPOGPOGPOGPOG <b>AH</b>
(POG) <sub>n</sub> H	POGPOGPOGPOGPOGPOG <b>H</b>
(POG) <sub>10</sub>	POGPOGPOGPOGPOGPOGPOGPOGPOGPOG
(PPG) <sub>10</sub>	PPGPPGPPGPPGPPGPPGPPGPPGPPGPPGPPG

(ii) Charged peptides

A	PKGPKGPKGKOGPDGDOGDODGPKGPKG
APAH	PKGPKGPKGKOGPDGDOGDODG <b>PKGPKG<b>PAH</b></b>
AH	PKGPKGPKGKOGPDGDOGDODG <b>PKGPKG<b>AH</b></b>
AH	PKGPKGPKGKOGPDGDOGDODG <b>PKGPKG<b>H</b></b>
B	PDGDOGDODGDPGKOGPDGPDGPDGDOGDODG
BPAH	PDGDOGDODGDPGKOGPDGPDGPDG <b>PDGDOGDODG<b>PAH</b></b>
BAH	PDGDOGDODGDPGKOGPDGPDGPDG <b>PDGDOGDODG<b>AH</b></b>
BH	PDGDOGDODGDPGKOGPDGPDGPDG <b>PDGDOGDODG<b>H</b></b>
C	KOGPDPGDPGPKGPKGKOGKOGKOGKOGKOG
C <b>PAH</b>	KOGPDPGDPGPKGPKGKOGKOGKOG <b>KOG<b>PAH</b></b>
C <b>AH</b>	KOGPDPGDPGPKGPKGKOGKOGKOG <b>AH</b>
C <b>H</b>	KOGPDPGDPGPKGPKGKOGKOGKOG <b>H</b>

Designed metal-binding ligands and associated linkers shown in bold. O = 4R-hydroxyproline.

Peptide solutions were prepared in 10 mM Tris buffer pH = 7.4, with or without 150 mM NaCl and metal salts. Peptide concentrations in solution were estimated by measuring absorbance at 214 nm using  $\epsilon_{214} = 2200 \text{ M}^{-1} \text{ cm}^{-1}$ . After mixtures were prepared at room temperature, they were denatured at 80 °C for 30 min and annealed at 4 °C for at least 48 h.

Lyophilized calf-skin collagen Type I was provided by Elastin Products Company (Cat no.: C857). Lyophilized protein was directly dissolved in either acetic acid or Tris buffer (pH 7.2) with or without the addition of metal salts.

**Circular Dichroism (CD).** CD measurements were conducted using the Aviv model 420SF spectrophotometer equipped with a Peltier temperature controller. For wavelength spectra, measurements were made at every 0.5 nm step with an averaging time of 10 s at each wavelength. Scans were conducted from 190 to 260 nm at 5 °C. Observed ellipticity was converted to molar ellipticity by dividing raw values by the peptide concentration, number of residues, and cell path length. For temperature induced denaturation, ellipticity was measured at 225 nm for (POG)<sub>n</sub> and (PPG)<sub>n</sub> domain peptides, or at 223 nm for charged peptides. Unless otherwise specified, total peptide concentrations used were 0.2 mM. CD temperature denaturation profiles were smoothed using the Savitsky-Golay algorithm with 19 points and a third-order polynomial,<sup>59</sup> and melting temperatures assigned based on extrema of the first derivative.

**Dynamic Light Scattering (DLS).** DLS measurements were performed using a Zetasizer Nano ZS (Malvern Instruments, UK). Data were collected with a 3 mW He–Ne laser at a 633 nm wavelength. This unit collects back scattered

light at an angle of 173° and contains a built-in Peltier element temperature controller. Autocorrelation functions were determined from the average of three correlation functions, with an acquisition time of 2 min per correlation function. Reported viscosity values<sup>60</sup> were used for the hydrodynamic radius calculation. A detailed description of the DLS instrumental setup and data analysis methods can be found elsewhere.<sup>61,62</sup>

**Isothermal Titration Calorimetry (ITC).** Isothermal titration calorimetry (ITC) measurements were carried out at 25 °C using an ITC 200 calorimeter (GE Biosciences, Piscataway, NJ). All solutions were filtered through 0.2 μm syringe filters and degassed for 5 min prior to measurement. Aliquots (35–40 μL) of 1.67 mM ZnCl<sub>2</sub> were injected from a 1000 rpm rotating syringe into a 0.2 mL sample cell containing 0.167 mM trimer (0.5 mM monomer) with a 180 s delay between injections. Each titration experiment was accompanied by the corresponding control experiment in which ZnCl<sub>2</sub> was injected into a solution of buffer alone. Each injection generated a heat burst curve (μcal/s versus s), the area under which was determined by integration using Origin version 7.0 software (OriginLab Corp., Northampton, MA), to obtain a measure of the heat associated with that injection. The measure of the heat associated with each ZnCl<sub>2</sub>-buffer injection, as estimated using a linear regression analysis of the integrated data, was subtracted from that of the corresponding heat associated with each ZnCl<sub>2</sub>-peptide injection to yield the heat of ZnCl<sub>2</sub> binding for that injection. Following removal of the point corresponding to the first low volume injection, the buffer-corrected ITC profiles for the binding of each experiment were fit with a model for one set of binding sites.

## RESULTS AND DISCUSSION

**Metal Binding Enhances Stability.** We previously designed a series of collagen peptides specifically intended to form an A:B:C heterotrimer.<sup>56</sup> In order to design a metal binding site that targets an ABC heterotrimer, we developed a model that took advantage of the one amino acid stagger of A relative to B, and B to C. Starting with the assumption that the designed register ABC is the correct one, adding *x*xH, *x*H and H linkers to A, B and C, respectively, should form a blunted-end design (Figure 1). Linkers were modeled onto the high-resolution structure of a [(POG)<sub>10</sub>]<sub>3</sub> CMP as *x*-*x*-His, *x*-His, and His for the leading, central, and lagging strands. Backbone torsions of *x* and histidine, and side chain rotamers of histidine were sampled using the modeling platform protCAD<sup>63</sup> for those that formed a tetrahedral His<sub>3</sub>-metal site. The optimal conformation identified in the linker sampling specified all *x* positions in an α-helical conformation ( $\phi \approx -60^\circ$ ,  $\psi \approx -45^\circ$ ). Linker amino acids were chosen based on known backbone conformation preferences. Proline, which is favored at the beginning of α-helices,<sup>64</sup> and alanine, which stabilizes the α-helix,<sup>65</sup> were incorporated to optimize the target linker conformation, such that the imidazole side chains presented a preorganized tetrahedral metal binding site. Structures were minimized in AMBER using the ff99sb force field<sup>66</sup> plus parameters for a zinc pseudoatom.<sup>67</sup> Pro-Ala-His (PAH), Ala-His (AH), and His (H) were appended to the C-terminus of A, B, and C peptides respectively to obtain A<sub>PAH</sub>, B<sub>AH</sub>, and C<sub>H</sub> peptides.

Metal binding linkers in an α-helical conformation should not extend the interchain hydrogen bonding network of the triple-helix and were not expected to significantly perturb stability except in the presence of a coordinated metal. CD

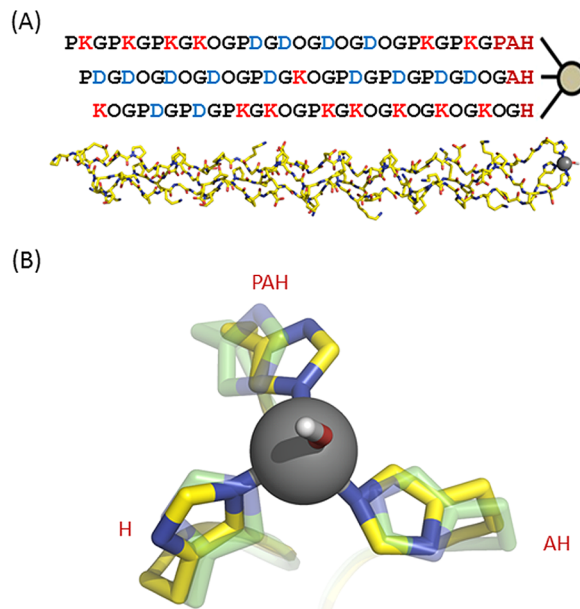


**Figure 1.** Blunt-end design of a collagen metalloprotein: (A) model of peptides containing histidines at the C-terminus coordinating zinc, to stabilize the heterotrimer. (B) An initial configuration built using protCAD (green) and minimized with AMBER (yellow) to model the heterotrimeric zinc-histidine site.

wavelength spectra and thermal denaturation profiles of the A<sub>PAH</sub>:B<sub>AH</sub>:C<sub>H</sub> heterotrimer showed triple-helical structure and comparable stability to the original A:B:C (Figure 2). Differences of ~2–3 °C for the A:B:C system from the previously published  $T_m$  values<sup>56</sup> were due to the use of a Tris-buffer system instead of phosphate to allow for metal binding studies to be performed. In both peptide sets, two transitions were observed in the absence of NaCl, corresponding to potential multiple registers of association or the formation of competing species with lower thermal stability. Increased ionic strength decreased the stability of both A:B:C and A<sub>PAH</sub>:B<sub>AH</sub>:C<sub>H</sub> heterotrimers and eliminated one of the transitions (Figure S2) consistent with our previous characterization of the A:B:C heterotrimer.<sup>56</sup>

Addition of the histidine ligand and associated linkers did not perturb heterospecificity of triple-helix folding. Ten combinations of the histidine-containing peptides (A<sub>PAH</sub>:B<sub>AH</sub>:C<sub>H</sub>, 2A<sub>PAH</sub>:B<sub>AH</sub>, A<sub>PAH</sub>:2B<sub>AH</sub>, 2A<sub>PAH</sub>:C<sub>H</sub>, A<sub>PAH</sub>:2C<sub>H</sub>, 2B<sub>AH</sub>:C<sub>H</sub>, B<sub>AH</sub>:2C<sub>H</sub>, 3A<sub>PAH</sub>, 3B<sub>AH</sub>, 3C<sub>H</sub>) were prepared in the presence of ZnCl<sub>2</sub>, of which only A<sub>PAH</sub>:B<sub>AH</sub>:C<sub>H</sub> formed a triple-helix (Figure 3, S3A). Inclusion of ZnCl<sub>2</sub> up to 2.0 mM stabilized the His<sub>3</sub> containing heterotrimer. Zinc concentrations greater than 2.0 mM decreased structure and stability of A<sub>PAH</sub>:B<sub>AH</sub>:C<sub>H</sub>. This is presumably due to screening of interchain electrostatic interactions upon increasing ionic strength, as was previously observed for the unmodified peptides.<sup>56</sup> To examine whether stability enhancements could be caused by nonspecific metal–salt interactions, we titrated CaCl<sub>2</sub>, which does not interact strongly with histidine, into the A<sub>PAH</sub>:B<sub>AH</sub>:C<sub>H</sub> mixture. The lack of Ca(II) binding to the heterotrimer was consistent with specific coordination of imidazoles. At 4-fold lower total peptide concentrations (0.05 mM), the A<sub>PAH</sub>:B<sub>AH</sub>:C<sub>H</sub> heterotrimer was unfolded. Under these conditions, inclusion of Zn(II) induced folding of the triple-helix and enhanced stability in a concentration-dependent manner (Figure S3B).

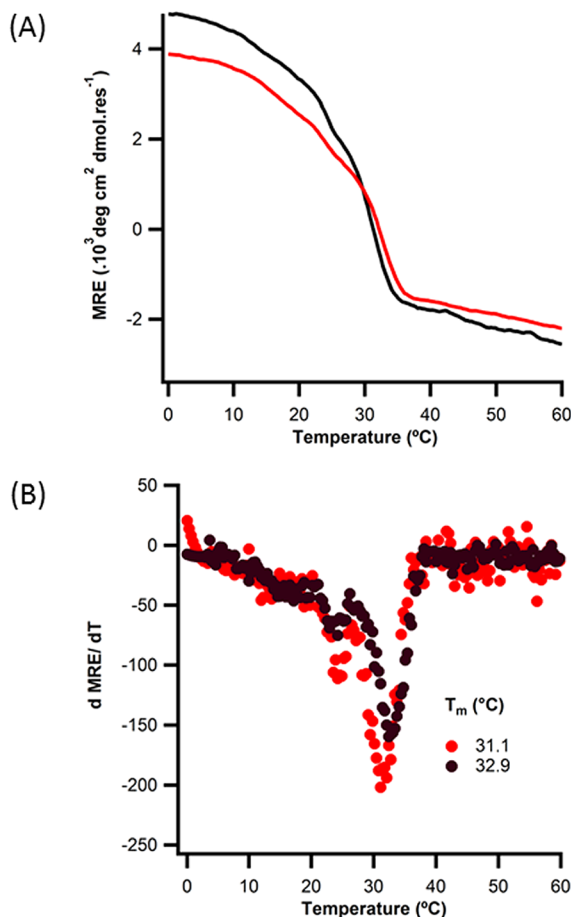


**Figure 2.** Effect of linker on structure and stability of the A:B:C heterotrimer. (A) CD temperature-melting curves monitored at 223 nm of 0.2 mM ABC (red) and A<sub>PAH</sub>:B<sub>AH</sub>:C<sub>H</sub> (black) collagen like peptides in phosphate buffer without salt; (B) respective first derivative plots. Effect of increasing ionic strength shown in Figure S2.

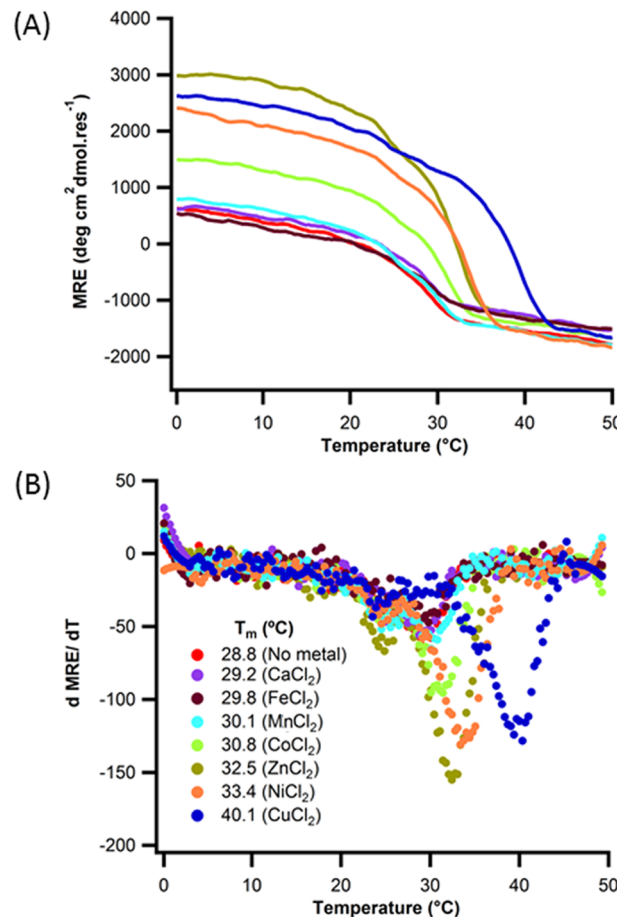


**Figure 4.** Metal-dependent stabilization of the triple helix. (A) Circular dichroism temperature melting curves monitored at 223 nm of 0.18 mM A<sub>PAH</sub>:B<sub>AH</sub>:C<sub>H</sub> heterotrimer peptide in 10 mM Tris buffer, pH = 7.4, 150 mM NaCl in 0.36 mM concentration of different metals (B) their respective first derivative plots.

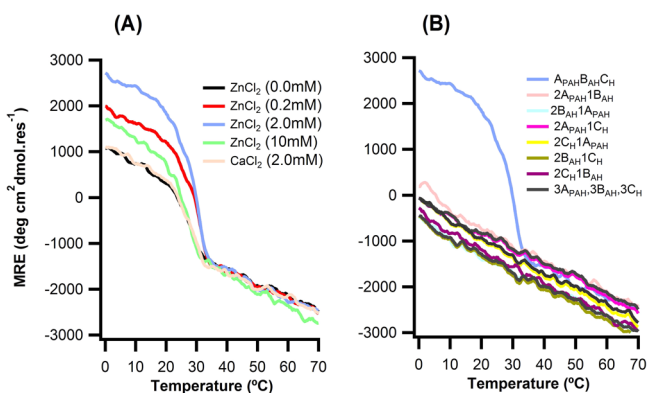


**Figure 3.** abc-type heterotrimer required for metal binding. Circular dichroism temperature melting curves monitored at 223 nm of (A) A<sub>PAH</sub>:B<sub>AH</sub>:C<sub>H</sub> heterotrimer peptide in 10 mM Tris buffer, pH = 7.5, 150 mM NaCl with varying concentration of ZnCl<sub>2</sub> or CaCl<sub>2</sub>. (B) All 10 possible combination of A<sub>PAH</sub>, B<sub>AH</sub>, and C<sub>H</sub> in 10 mM Tris buffer, 150 mM NaCl, 2 mM ZnCl<sub>2</sub>.

**Effect of Metal Species on the Stability.** We measured the stability of A<sub>PAH</sub>:B<sub>AH</sub>:C<sub>H</sub> in the presence of metal salts: ZnCl<sub>2</sub>, CaCl<sub>2</sub>, CoCl<sub>2</sub>, MnCl<sub>2</sub>, FeCl<sub>2</sub>, NiCl<sub>2</sub>, and CuCl<sub>2</sub>. No significant changes in structure or stability were seen with Mn(II), Fe(II), and Ca(II) (Figure 4). Addition of Co(II)

showed a slight increase in MRE and stability. Ni(II) and Zn(II) showed more pronounced effects, while addition of Cu(II) had the largest increase on stability,  $\Delta T_m = 12^{\circ}\text{C}$ , consistent with previous reports of copper and zinc binding and stabilization of histidine containing peptides.<sup>36</sup> Metal binding affinities agreed with the expected Irving–Williams series for imidazole: Ca<sup>2+</sup> < Mn<sup>2+</sup> < Fe<sup>2+</sup> < Co<sup>2+</sup> < Ni<sup>2+</sup> < Cu<sup>2+</sup> < Zn<sup>2+</sup>.<sup>68</sup>

**Testing the Blunt-Ended Model.** We tested the blunt-end design hypothesis using two approaches. First, a homotrimeric system was used to determine whether a blunt-end site was essential for metal binding. Homotrimers can only form staggered binding sites and might therefore be expected to poorly coordinate metal. Second, we wanted to assess whether the blunt-ended site was the optimal linker configuration. To determine this, we took advantage of the heterospecific association of A:B:C to sample linker configurations the metal binding.

A blunt-ended structure cannot form in a homotrimeric system when each chain has the same linker, instead creating a metal binding site where each histidine is staggered by one amino acid relative to the next. Thus, constructing homotrimers with various linkers allows us to examine the flexibility of the metal binding site. The H, AH, and PAH linkers were added to the C-terminus of a homotrimer forming (POG)<sub>7</sub> domain. All species formed stable triple-helical structures with and without

$\text{ZnCl}_2$  (Figure S4). Addition of  $\text{ZnCl}_2$  to  $(\text{POG})_7\text{AH}$  and  $(\text{POG})_7\text{PAH}$  increased stability by approximately 7 °C (Figure S5, Table S1). However, only a marginal effect was observed for  $(\text{POG})_7\text{H}$  stability, about 2 °C. Homotrimers did not bind  $\text{Ca}(\text{II})$ , indicating that specific imidazole coordination was required to enhance stability. To model the zinc-mediated stability, relevant homotrimer structures were computed and optimized. The extent to which each homotrimer model could geometrically adopt a metal binding conformation was consistent with the observed stability enhancement (PAH, AH > H). Affinities assessed by ITC (Figure S5) exhibit the same trend as stability measured by CD and calculated binding scores (Table S1).

Given that  $(\text{POG})_7\text{H}$  could not be modeled to adopt a metal binding site, it was suspected the small increase in stability could be due to the metal coordination by multiple triple-helices. Similar behavior was observed in related designed peptides containing a histidine at both N- and C-terminal ends of the sequence (i.e., HG(PPG)<sub>9</sub>GH),<sup>36</sup> where metal binding enhanced fold stability and drove higher-order assembly. Dynamic light scattering measurements (DLS) were conducted for all three homotrimer peptides in increasing concentrations of  $\text{ZnCl}_2$ . DLS measures the Brownian motion of the particle and correlates it to its size. DLS confirmed the formation of higher order structures for  $(\text{POG})_7\text{H}$  upon addition of zinc, suggesting more than one peptide trimer was required to form a complete binding site. Larger species were not observed for  $(\text{POG})_7\text{AH}$  or  $(\text{POG})_7\text{PAH}$  upon addition of zinc (Figure S6). This suggests that the increase in stability driven by intrahelical formation of a  $\text{His}_3$ -metal site precludes multiple helical elements interacting with the same metal ion. In the case of  $(\text{POG})_7\text{H}$ , formation of an intrahelical metal site requires significant conformational strain, instead promoting multi-helical metal assemblies, such as those in related systems where such behavior is intentionally designed.<sup>36,37</sup>

The homotrimer results clearly demonstrated that forming a blunt-ended site is not an essential requirement for metal binding. However, the blunt-end may still be the optimal configuration, requiring minimal rearrangement of the linker conformation to coordinate metal. A blunt-ended metal site can only be constructed using a heterotrimer where the leading, middle, and lagging strands are augmented with PAH, AH, and H linkers, respectively. To systematically evaluate the relationship between binding site geometry and metal binding, we generated a library of peptide + linker variants:  $\text{A}_H$ ,  $\text{A}_{AH}$ ,  $\text{A}_{PAH}$ ,  $\text{B}_H$ ,  $\text{B}_{AH}$ ,  $\text{B}_{PAH}$ ,  $\text{C}_H$ ,  $\text{C}_{AH}$ ,  $\text{C}_{PAH}$ . From these nine peptides, one could potentially assemble 27 ( $3 \times 3 \times 3$ ) linker sequence permutations on an A:B:C heterotrimer. We focused on a subset of these to determine whether a blunt-end design provided an optimal metal binding site.

We first examined the three cases where all peptide chains A, B, and C had the same linker, resulting in a staggered binding site:  $\text{A}_H:\text{B}_H:\text{C}_H$ ,  $\text{A}_{AH}:\text{B}_{AH}:\text{C}_{AH}$ , and  $\text{A}_{PAH}:\text{B}_{PAH}:\text{C}_{PAH}$ . These linker geometries would be most comparable to the  $(\text{POG})_7$  homotrimer experiments—i.e., they are incapable of creating a blunt-ended site. As seen in the homotrimer, the PAH linker increased the baseline stability of the heterotrimer by a few degrees Celsius relative to the AH and H linkers (Table 1, Figure 5). Addition of Zn(II) and Cu(II) increased stability in all cases. Unlike the homotrimer  $(\text{POG})_7\text{H}$ ,  $\text{A}_H:\text{B}_H:\text{C}_H$  showed enhanced stability on par with the other two linkers. Together, these two observations suggest that heterotrimers show increased conformational flexibility at the C-terminus, presum-

**Table 1. Melting Temperature ( $T_m$ ) of Mixture of Peptides A, B, C with Different Combinations of Ligands PAH, AH, and H in the Absence of Metal and in the Presence of 2 mM  $\text{ZnCl}_2$  or  $\text{CuCl}_2$**

peptides	$T_m$ (°C)	$\Delta T_m$ (°C) <sup>a</sup>		computed binding score <sup>b</sup>
	no metal	+Zn(II)	+Cu(II)	
same linkers				
$\text{A}_H:\text{B}_H:\text{C}_H$	27.5	+3.5	+8.3	13858
$\text{A}_{AH}:\text{B}_{AH}:\text{C}_{AH}$	27.4	+4.3	+11.0	1007
$\text{A}_{PAH}:\text{B}_{PAH}:\text{C}_{PAH}$	29.5	+3.3	+9.9	5744
unique linkers				
$\text{A}_{PAH}:\text{B}_{AH}:\text{C}_H^c$	28.8	+2.6	+10.0	1283
$\text{A}_{PAH}:\text{B}_H:\text{C}_{AH}$	28.2	+1.9	+8.8	4886
$\text{A}_{AH}:\text{B}_{PAH}:\text{C}_H$	28.1	+4.7	+9.2	607
$\text{A}_{AH}:\text{B}_H:\text{C}_{PAH}$	28.2	+4.2	+10.5	499
$\text{A}_H:\text{B}_{AH}:\text{C}_{PAH}$	28.2	+4.5	+9.2	2550
$\text{A}_H:\text{B}_{PAH}:\text{C}_{AH}$	29.1	+1.7	+8.9	10380

<sup>a</sup> $\Delta T_m$  (°C) =  $T_m$  (metal) –  $T_m$  (no metal) <sup>b</sup>Linkers were modeled at the C-terminus using the structure of an idealized (PPG)<sub>10</sub> triple-helix, assuming three peptides are listed in order of leading, middle, and lagging strand. Values for the best ligand configuration are indicated here. For all ligand configurations, see Tables S2 and S3. <sup>c</sup>Corresponds to the blunt-ended design if association state is ABC.

ably due to the lower content of rigid imino acids relative to  $(\text{POG})_7$ . Increased flexibility may decrease the coupling between triple-helix stability and metal binding, and reduce the effect of linker length on accommodating a metal binding site at the C-terminus of the triple helix.

Next, we examined the six states where each chain has a different linker ( $\text{A}_{PAH}:\text{B}_{AH}:\text{C}_H$ ,  $\text{A}_{AH}:\text{B}_{PAH}:\text{C}_H$ ,  $\text{A}_{AH}:\text{B}_H:\text{C}_{PAH}$ ,  $\text{A}_{PAH}:\text{B}_H:\text{C}_{AH}$ ,  $\text{A}_H:\text{B}_{AH}:\text{C}_{PAH}$ ,  $\text{A}_H:\text{B}_{PAH}:\text{C}_{AH}$ ), that could potentially form a blunt-ended design. If A:B:C associates into one unique state and the blunt-end site is optimal for metal binding, one of these six combinations should have a detectably higher stability than the other five. The composition of the heterotrimer is known, but the register of the three chains is not.<sup>56</sup> As noted previously, in the absence of salt two melting transitions are observed, indicating that multiple registers may occur. Of the possible associations states: the target ABC and competing BCA, CAB are the most likely species given that these three are predicted to form the highest number of favorable charge pair interactions. CBA, BAC, and ACB are unlikely to be formed as these have primarily repulsive interchain interactions with significantly lower computed interaction energies.<sup>56</sup>

The six mixtures each formed triple-helical structures with equivalent stabilities in the absence of metal (Table 1, Figure S7). While addition of either Zn(II) or Cu(II) stabilized the triple-helix in all cases, no one state stood out from the other five as having the highest degree of metal induced stabilization. Furthermore, the observed stability increases were within the same range as those for heterotrimers where each chain had the same linker. This indicates that linker length exerts minimal control on metal binding site affinity and that the blunt-end design as implemented is not sufficient to discriminate the correct register of A:B:C. In natural proteins where binding sites are in loops or other disordered regions, the strong metal–ligand interactions can remodel flexible regions of the protein to adopt a metal coordination site.<sup>69</sup> This appears to be the case at the termini of collagen as well. Another consideration is the

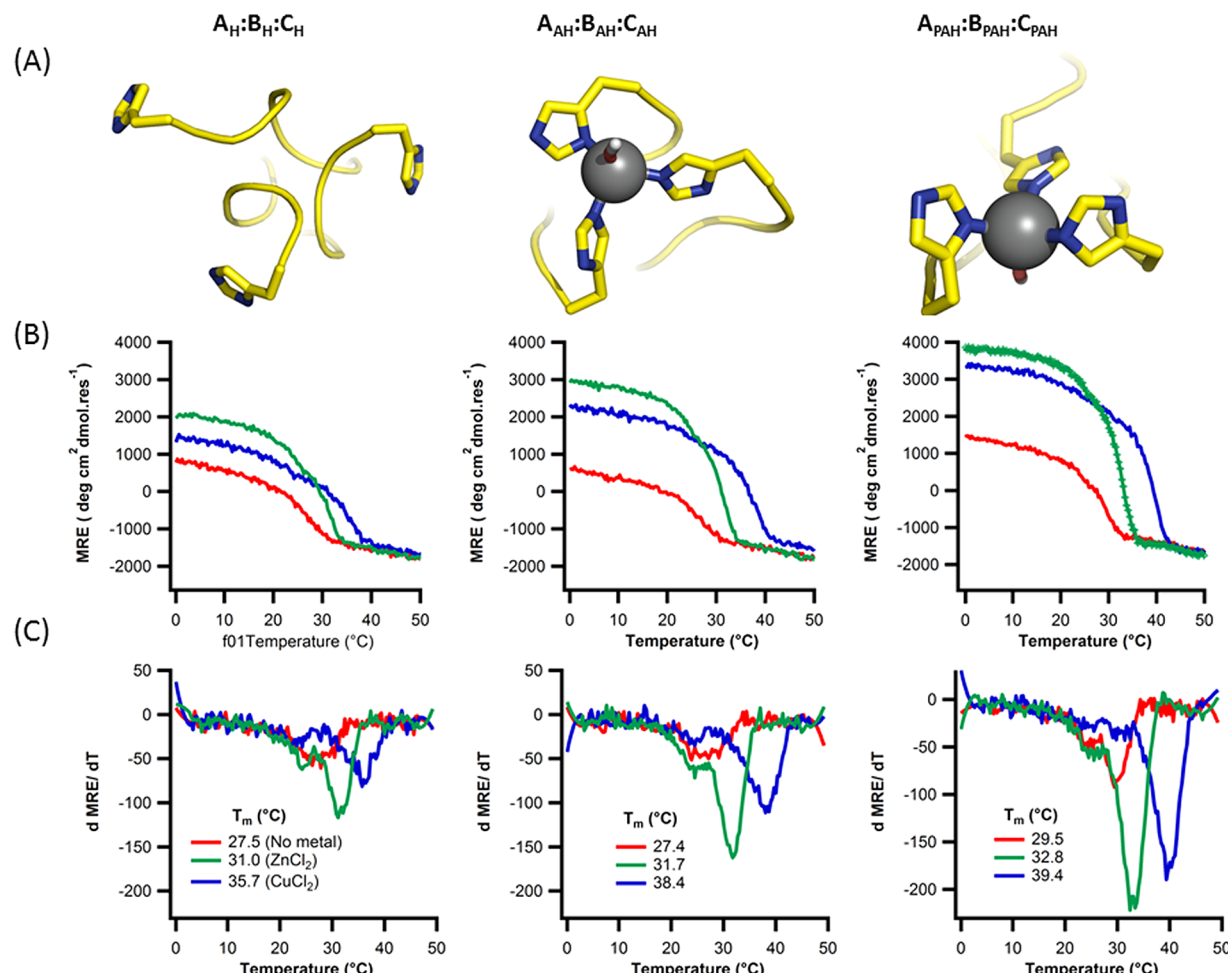


**Figure 5.** Modeling and characterization of heterotrimers with staggered metal binding sites:  $A_H:B_H:C_H$ ,  $A_{AH}:B_{AH}:C_{AH}$ , and  $A_{PAH}:B_{PAH}:C_{PAH}$  (A) atomic models constructed in protCAD and minimized in AMBER. In the case of  $A_H:B_H:C_H$  the mimized structure did not maintain a metal coordination competent geometry. (B) Thermal denaturation at 223 nm in 10 mM Tris buffer, pH = 7.4, 150 mM NaCl with (red) no metals (green) 0.36 mM of  $ZnCl_2$  and (blue) 0.36 mM  $CuCl_2$  (C) their respective first derivative plots.

presence of multiple transitions in many of the A:B:C-type peptide denaturation profiles, indicating that multiple species may be present. The resulting heterogeneity in binding site configurations may allow additional plasticity in metal coordination.

**Modeling of Potential Linker Configurations.** Calculating a metal affinity score using a combination of geometric constraints on ligand–metal interactions and standard intramolecular forces indicates other linkers can provide good scoring coordination sites (Table S3). The blunt-end structure has the best packing energy, but other linker configurations have more ideal metal–ligand geometries. The correlation between calculated and observed stabilities for the variants tested in Table 1 are modest ( $R^2 = 0.56$  for copper and 0.42 for zinc). More sophisticated modeling approaches that adequately treat both ligand–metal and intramolecular forces could potentially improve the correlation between calculated and observed metal affinities.

**Evidence for Sequence-Independent Mode of Cu(II) Binding to Triple-Helical Peptides.** It was expected that all three histidines would be required for metal binding in the other heterotrimer variants—this turned out to be the case for zinc (Figure 6). However, the addition of Cu(II) enhanced heterotrimer stability even when a complete His<sub>3</sub> site was

absent. Furthermore, no significant correlation was observed between the degree of stabilization of heterotrimer linker combinations in the presence of Zn(II) versus Cu(II) (Table 1). This suggested that copper binds to the collagen peptides through an alternative or additional mode.

We examined metal binding to the A:B:C heterotrimer without the inclusion of C-terminal histidine. Addition of Zn(II) did not affect stability (Figure 7), but the same concentration of Cu(II) salt raised the melting temperature by 5 °C. A, B, and C peptides have a high number of charged amino acids (Asp and Lys) which were designed to form networks of stabilizing charge pairs along the helix axis.<sup>56</sup> To examine whether some of these groups may also be providing unanticipated binding sites, we examined neutral homotrimers (POG)<sub>10</sub> and (PPG)<sub>10</sub>, also lacking C-terminal histidine groups. Again, enhancement of stability was observed in the presence of copper, but zinc had no effect (Figure 8). The only competent metal ligands remaining in these proline-rich peptides were the backbone amides and carboxylates of peptide termini. The parallel orientation of the triple-helix chains brings together three amines or carboxylates in potentially favorable geometries for metal coordination. Capping the ends of the triple-helix by acetylation of the N-terminus and amidation of the C-terminus of (POG)<sub>10</sub>, giving Ac-(POG)<sub>10</sub>-NH<sub>2</sub>, resulted in a peptide that

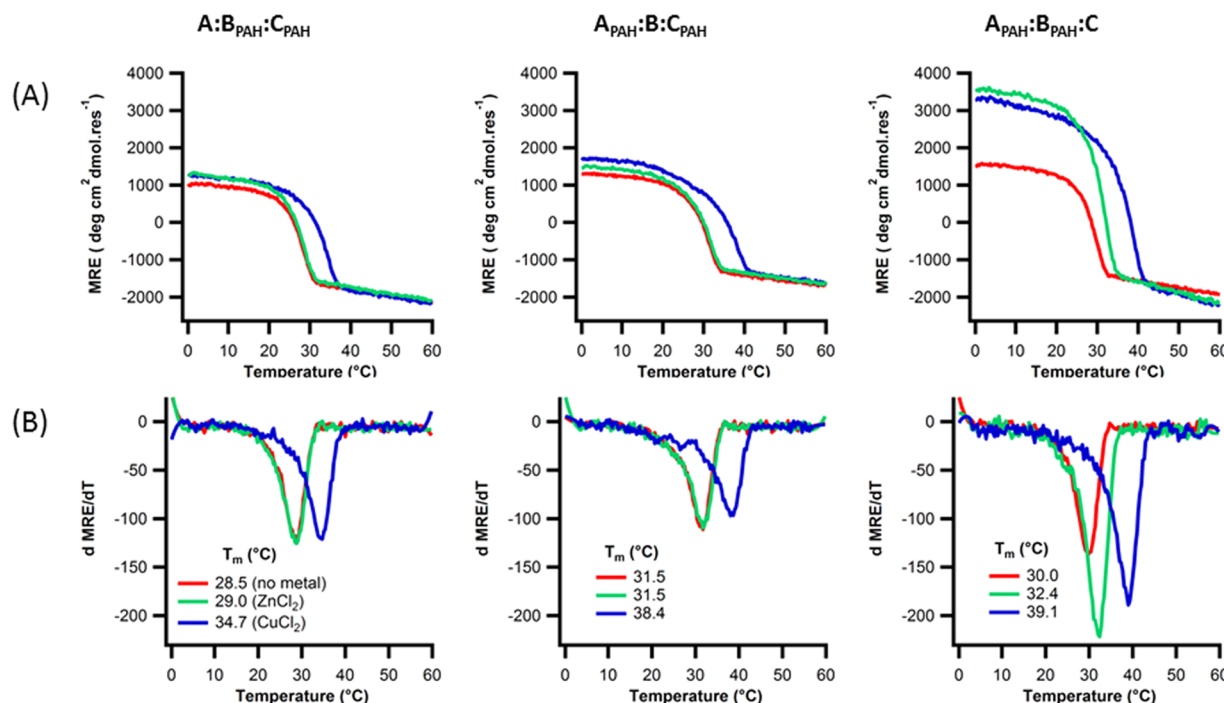


**Figure 6.** Metal-induced stabilization in the presence of incomplete binding sites. (A) Thermal denaturation at 223 nm in 10 mM Tris buffer, pH = 7.4, 150 mM NaCl with (red) no metals (green) 0.36 mM of ZnCl<sub>2</sub> and (blue) 0.36 mM CuCl<sub>2</sub> (B) their respective first derivative plots.

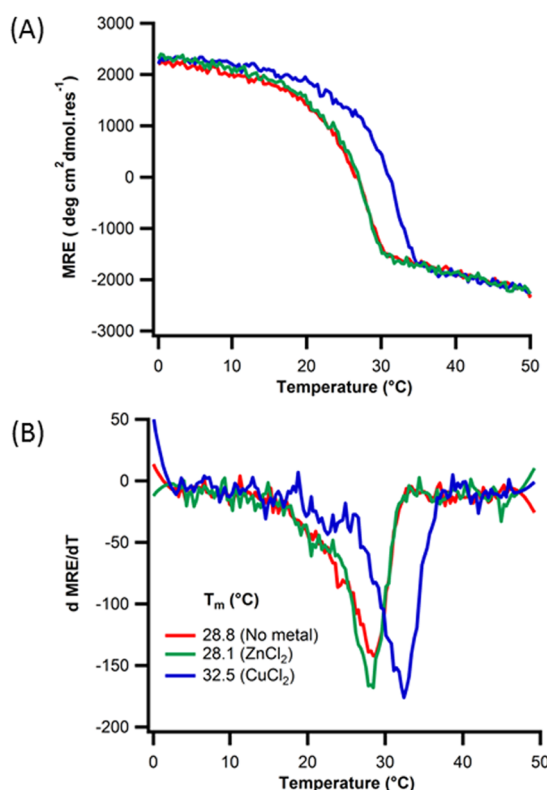


**Figure 7.** Metal binding to histidine-lacking heterotrimers. (A) CD temperature melting curves monitored at 223 nm of 0.18 mM A:B:C heterotrimer peptide in 10 mM Tris buffer, pH = 7.4, 150 mM NaCl in (red) no metal (green) 0.36 mM ZnCl<sub>2</sub>, (blue) 0.36 mM CuCl<sub>2</sub> (B) their respective first derivative plots.

did not increase in stability upon addition of copper. This suggested that one of the two termini was forming a secondary copper binding site.

To identify on which end of the triple-helix copper binding occurs, we synthesized a singly capped variant of (POG)<sub>7</sub>, which was only acetylated on the N-terminus: Ac-(POG)<sub>7</sub>-OH. This modification prevented copper binding, indicating that the N-termini of triple-helices were responsible for coordinating copper (Figure 9). The observed stabilization of A<sub>PAH</sub>:B<sub>PAH</sub>:C by Cu(II) was due to the presence of two copper sites, one at the N-terminus and the other at the His<sub>3</sub> site.

Provided copper binds to backbone amines at the N-terminus of the triple-helix in a sequence-independent manner, it was thought that similar binding would be observed to natural collagen. We measured the thermal denaturation of calf-skin Type I collagen in the absence and presence of a series of metals. Similar to the peptide result, copper raised the T<sub>m</sub> of collagen by ~5 °C (Figure 10). No effect was seen in the presence of equivalent concentrations of zinc or calcium. Addition of copper did not perturb the oligomeric state of collagen as measured by DLS (Figure S8), suggesting stabilization through intrahelical interactions. It should be noted that animal-extracted collagen has a short, nontriple-helical, N-terminal telopeptide, which should not present the same ligand configuration as the peptides. Therefore, the mode of copper binding may be different between natural collagen and peptide mimetics.

## CONCLUSIONS

The polyproline II conformation of the triple-helix is a challenging structural context in which to design metal binding sites. This is particularly evident at the termini, where chain flexibility hinders the design of a specific, structurally unique binding site. Although the protCAD software platform used here was previously successful in developing metal binding  $\alpha$ -helix and  $\beta$ -sheet proteins,<sup>70,71</sup> collagen presented a novel design challenge due to its flexibility. One of the advantages of putting the binding sites at the flexible region of a protein is

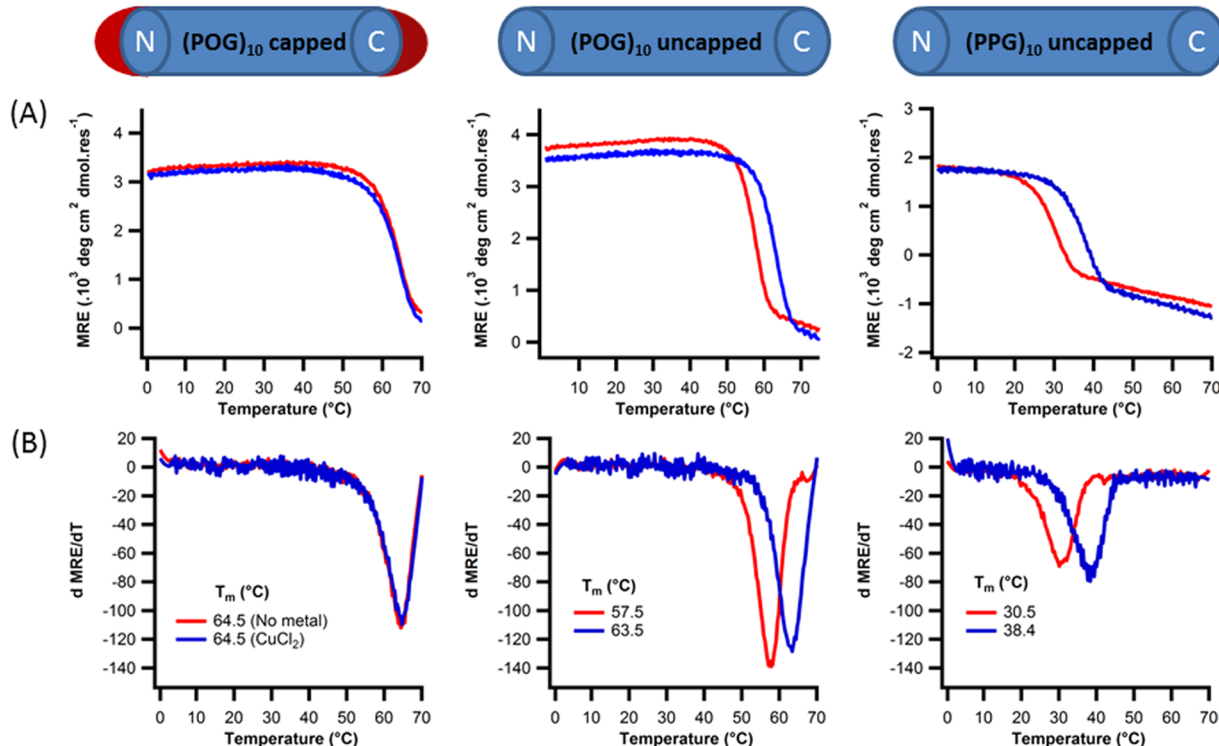


**Figure 8.** Copper binding to neutral collagen model peptides. (A) Circular dichroism temperature melting curves monitored at 225 nm of 0.2 mM (left) capped (POG)<sub>10</sub>; (middle) uncapped (POG)<sub>10</sub>; (right) uncapped (PPG)<sub>10</sub> peptide in 10 mM Tris buffer, pH = 7.4, 150 mM NaCl with (red) no metal, (blue) 0.2 mM CuCl<sub>2</sub> (B) their respective first derivative plots.

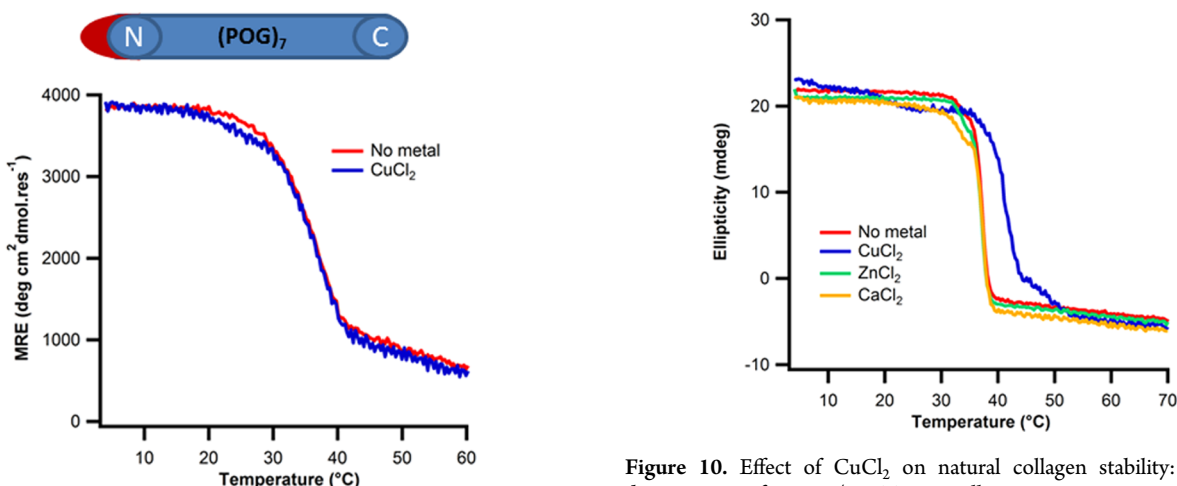


**Figure 9.** Sequence-independent binding of copper to the N-terminus of the triple helix. Circular dichroism temperature melting curves monitored at 225 nm of 0.2 mM N-terminus blocked (POG)<sub>7</sub> with (blue) and without (red) CuCl<sub>2</sub>. No change in melting temperature was observed in the presence of CuCl<sub>2</sub>.

that the ligands can adjust to bind the metals in their preferred geometry.<sup>69,72</sup> Constraining the linker geometry to promote formation of a specific heterotrimeric blunt-ended metal binding site proved to be very difficult. This work highlights the potential importance of multistate design<sup>73</sup> in collagen engineering where both stability of the target and specificity against competing states are explicitly considered.<sup>74</sup> Multistate design protocols have been applied at the sequence modeling level to collagen. To achieve metal binding specificity, we

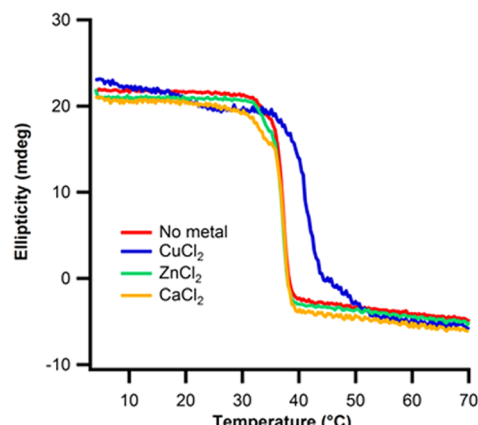


**Figure 10.** Effect of CuCl<sub>2</sub> on natural collagen stability: Thermal denaturation of 0.4 mg/mL Type I collagen at 222 nm in 10 mM Tris buffer, pH = 7.4, (red) no metals, (blue) 1.2 mM CuCl<sub>2</sub>, (green) 1.2 mM ZnCl<sub>2</sub>, (orange) 1.2 mM CaCl<sub>2</sub>.

expect similar approaches to be useful in atomistic design protocols as well.

There are now several strategies for stabilizing the collagen triple-helix using terminal augments. Natural pro-collagens contain N- and/or C-terminal globular noncollagenous domains that are responsible for directing oligomerization prior to their cleavage from the triple-helix. This has inspired the design of synthetic protein augments such as a trimeric foldon taken from bacteriophage fibrin<sup>75,76</sup> or trimeric coiled coils<sup>77</sup> which mimic the adjacent V-domain of bacterial collagens.<sup>78,79</sup> Metal binding sites have been used to engineer self-assembling systems where assembly is gated by a metal switch.<sup>34,37–40,80</sup> Metal binding combined with heterospecific

interstrand interactions provide an expanding set of tools for controlling the chemical and physical properties of collagen-derived biomaterials.

Copper binding to the N-termini of proteins has been previously observed and in some cases shown to depend on its acetylation state.<sup>81</sup> Cu(II) has a high affinity for proline,<sup>82</sup> and the close proximity of the three N-termini in the triple helix may provide an entactic state favoring binding. Copper is necessary for catalytic activity of lysyl-oxidase, which cross-links animal collagen, contributing to its mechanical strength. This work suggests that copper may have additional effects on collagen matrices that may manifest in metal trafficking disorders such as Wilson's disease. Characterizing the specific interactions between copper and collagen may further our understanding of the etiology of metal-trafficking disorders and the engineering of collagen-based biomaterials.<sup>83</sup> Toxic metals such as chromium and aluminum affect the stability and higher-order structure of animal-extracted collagen,<sup>10–12</sup> and are used in leather processing as tanning agents. On the basis of the observed broad spectrum effects of copper on many collagen-like systems, CMPs could be used as models to understand how other metals impact collagen structure in both industrial and biological contexts.

## ■ ASSOCIATED CONTENT

### Supporting Information

The Supporting Information is available free of charge on the ACS Publications website at DOI: [10.1021/acs.biochem.5b00502](https://doi.org/10.1021/acs.biochem.5b00502).

Description of computational modeling of collagen structure, additional modeling and experimental data figures and tables, and peptide purification and characterization are including the supplemental Supporting Information ([PDF](#))

## ■ AUTHOR INFORMATION

### Corresponding Author

\*E-mail: [nanda@cabm.rutgers.edu](mailto:nanda@cabm.rutgers.edu).

### Funding

V.N. acknowledges funding from NSF DMR-0907273, NIH DP2-OD-006478-1, and NIH R01-GM-08994-01 to carry out this work. A.S.P. acknowledges support from Department of Science & Technology (DST-SERB) - SB/FTP/PS-073/2014, India to carry out this work. D.I.S. acknowledges support from the NSF CAREER Award: ARRA-CBET0846328. K.E.D. was supported by the Rutgers Biotechnology Training Grant from the NIH: ST32GM008339-20.

### Notes

The authors declare no competing financial interest.

## ■ ACKNOWLEDGMENTS

We thank Drs. Christopher Barbieri and Ann Stock, CABM, Piscataway, NJ, for assistance with ITC measurements.

## ■ REFERENCES

- (1) DeGrado, W. F., Summa, C. M., Pavone, V., Nastri, F., and Lombardi, A. (1999) De novo design and structural characterization of proteins and metalloproteins. *Annu. Rev. Biochem.* **68**, 779–819.
- (2) Kennedy, M. L., and Gibney, B. R. (2001) Metalloprotein and redox protein design. *Curr. Opin. Struct. Biol.* **11**, 485–490.
- (3) Lu, Y., Yeung, N., Sieracki, N., and Marshall, N. M. (2009) Design of functional metalloproteins. *Nature* **460**, 855–862.

- (4) Clarke, N. D., and Yuan, S. M. (1995) Metal search: a computer program that helps design tetrahedral metal-binding sites. *Proteins: Struct., Funct., Genet.* **23**, 256–263.

- (5) Klemba, M., Gardner, K. H., Marino, S., Clarke, N. D., and Regan, L. (1995) Novel metal-binding proteins by design. *Nat. Struct. Biol.* **2**, 368–373.

- (6) Benson, D. E., Wisz, M. S., and Hellinga, H. W. (2000) Rational design of nascent metalloenzymes. *Proc. Natl. Acad. Sci. U. S. A.* **97**, 6292–6297.

- (7) Brodin, J. D., Ambroggio, X. I., Tang, C., Parent, K. N., Baker, T. S., and Tezcan, F. A. (2012) Metal-directed, chemically tunable assembly of one-, two- and three-dimensional crystalline protein arrays. *Nat. Chem.* **4**, 375–382.

- (8) Dieckmann, G. R., McRorie, D. K., Lear, J. D., Sharp, K. A., DeGrado, W. F., and Pecoraro, V. L. (1998) The role of protonation and metal chelation preferences in defining the properties of mercury-binding coiled coils. *J. Mol. Biol.* **280**, 897–912.

- (9) Handel, T. M., Williams, S. A., and DeGrado, W. F. (1993) Metal ion-dependent modulation of the dynamics of a designed protein. *Science* **261**, 879–885.

- (10) Gayatri, R., Sharma, A. K., Rajaram, R., and Ramasami, T. (2001) Chromium(III)-induced structural changes and self-assembly of collagen. *Biochem. Biophys. Res. Commun.* **283**, 229–235.

- (11) Wu, B., Mu, C. D., Zhang, G. Z., and Lin, W. (2009) Effects of Cr<sup>3+</sup> on the Structure of Collagen Fiber. *Langmuir* **25**, 11905–11910.

- (12) He, L. R., Cai, S. M., Wu, B., Mu, C. D., Zhang, G. Z., and Lin, W. (2012) Trivalent chromium and aluminum affect the thermo-stability and conformation of collagen very differently. *J. Inorg. Biochem.* **117**, 124–130.

- (13) Engel, J., Chen, H. T., Prockop, D. J., and Klump, H. (1977) The triple helix in equilibrium with coil conversion of collagen-like polytripeptides in aqueous and nonaqueous solvents. Comparison of the thermodynamic parameters and the binding of water to (L-Pro-L-Pro-Gly)<sub>n</sub> and (L-Pro-L-Hyp-Gly)<sub>n</sub>. *Biopolymers* **16**, 601–622.

- (14) Xu, Y., Bhate, M., and Brodsky, B. (2002) Characterization of the nucleation step and folding of a collagen triple-helix peptide. *Biochemistry* **41**, 8143–8151.

- (15) Bella, J., Eaton, M., Brodsky, B., and Berman, H. M. (1994) Crystal and molecular structure of a collagen-like peptide at 1.9 Å resolution. *Science* **266**, 75–81.

- (16) Kramer, R. Z., Bella, J., Brodsky, B., and Berman, H. M. (2001) The crystal and molecular structure of a collagen-like peptide with a biologically relevant sequence. *J. Mol. Biol.* **311**, 131–147.

- (17) Xu, Y., Hyde, T., Wang, X., Bhate, M., Brodsky, B., and Baum, J. (2003) NMR and CD spectroscopy show that imino acid restriction of the unfolded state leads to efficient folding. *Biochemistry* **42**, 8696–8703.

- (18) Bretscher, L. E., Jenkins, C. L., Taylor, K. M., DeRider, M. L., and Raines, R. T. (2001) Conformational stability of collagen relies on a stereoelectronic effect. *J. Am. Chem. Soc.* **123**, 777–778.

- (19) Holmgren, S. K., Bretscher, L. E., Taylor, K. M., and Raines, R. T. (1999) A hyperstable collagen mimic. *Chem. Biol.* **6**, 63–70.

- (20) Holmgren, S. K., Taylor, K. M., Bretscher, L. E., and Raines, R. T. (1998) Code for collagen's stability deciphered. *Nature* **392**, 666–667.

- (21) Shah, N. K., Ramshaw, J. A., Kirkpatrick, A., Shah, C., and Brodsky, B. (1996) A host-guest set of triple-helical peptides: stability of Gly-X-Y triplets containing common nonpolar residues. *Biochemistry* **35**, 10262–10268.

- (22) Persikov, A. V., Ramshaw, J. A., and Brodsky, B. (2005) Prediction of collagen stability from amino acid sequence. *J. Biol. Chem.* **280**, 19343–19349.

- (23) Persikov, A. V., Ramshaw, J. A., Kirkpatrick, A., and Brodsky, B. (2000) Amino acid propensities for the collagen triple-helix. *Biochemistry* **39**, 14960–14967.

- (24) Okuyama, K., Wu, G., Jiravanichanun, N., Hongo, C., and Noguchi, K. (2006) Helical twists of collagen model peptides. *Biopolymers* **84**, 421–432.

- (25) Summa, C. M., Lombardi, A., Lewis, M., and DeGrado, W. F. (1999) Tertiary templates for the design of diiron proteins. *Curr. Opin. Struct. Biol.* 9, 500–508.
- (26) Roth, W., and Heidemann, E. (1980) Triple Helix-Coil Transition of Covalently Bridged Collagen-Like Peptides. *Biopolymers* 19, 1909–1917.
- (27) Dolz, R., and Heidemann, E. (1986) Influence of Different Tripeptides on the Stability of the Collagen Triple Helix 0.1. Analysis of the Collagen Sequence and Identification of Typical Tripeptides. *Biopolymers* 25, 1069–1080.
- (28) Thakur, S., Vadolas, D., Germann, H. P., and Heidemann, E. (1986) Influence of Different Tripeptides on the Stability of the Collagen Triple Helix 0.2. An Experimental Approach with Appropriate Variations of a Trimer Model Oligotripeptide. *Biopolymers* 25, 1081–1086.
- (29) Germann, H. P., and Heidemann, E. (1988) A Synthetic Model of Collagen - an Experimental Investigation of the Triple-Helix Stability. *Biopolymers* 27, 157–163.
- (30) Fields, C. G., Lovdahl, C. M., Miles, A. J., Hageini, V. L. M., and Fields, G. B. (1993) Solid-Phase Synthesis and Stability of Triple-Helical Peptides Incorporating Native Collagen Sequences. *Biopolymers* 33, 1695–1707.
- (31) Goodman, M., Feng, Y. B., Melacini, G., and Taulane, J. P. (1996) A template-induced incipient collagen-like triple-helical structure. *J. Am. Chem. Soc.* 118, 5156–5157.
- (32) Koide, T., Yuguchi, M., Kawakita, M., and Konno, H. (2002) Metal-assisted stabilization and probing of collagenous triple helices. *J. Am. Chem. Soc.* 124, 9388–9389.
- (33) Lebruin, L. T., Banerjee, S., O'Rourke, B. D., and Case, M. A. (2011) Metal ion-assembled micro-collagen heterotrimers. *Biopolymers* 95, 792–800.
- (34) Przybyla, D. E., and Chmielewski, J. (2008) Metal-triggered radial self-assembly of collagen peptide fibers. *J. Am. Chem. Soc.* 130, 12610–12611.
- (35) Cai, W. B., Kwok, S. W., Taulane, J. P., and Goodman, M. (2004) Metal-assisted assembly and stabilization of collagen-like triple helices. *J. Am. Chem. Soc.* 126, 15030–15031.
- (36) Hsu, W., Chen, Y. L., and Horng, J. C. (2012) Promoting self-assembly of collagen-related peptides into various higher-order structures by metal-histidine coordination. *Langmuir* 28, 3194–3199.
- (37) Pires, M. M., and Chmielewski, J. (2009) Self-assembly of collagen peptides into microflobettes via metal coordination. *J. Am. Chem. Soc.* 131, 2706–2712.
- (38) Pires, M. M., Przybyla, D. E., and Chmielewski, J. (2009) A metal-collagen peptide framework for three-dimensional cell culture. *Angew. Chem., Int. Ed.* 48, 7813–7817.
- (39) Przybyla, D. E., and Chmielewski, J. (2010) Metal-triggered collagen peptide disk formation. *J. Am. Chem. Soc.* 132, 7866–7867.
- (40) Pires, M. M., Lee, J., Ernenwein, D., and Chmielewski, J. (2012) Controlling the morphology of metal-promoted higher ordered assemblies of collagen peptides with varied core lengths. *Langmuir* 28, 1993–1997.
- (41) Rubert Perez, C. M., Panitch, A., and Chmielewski, J. (2011) A collagen peptide-based physical hydrogel for cell encapsulation. *Macromol. Biosci.* 11, 1426–1431.
- (42) Gauba, V., and Hartgerink, J. D. (2008) Synthetic collagen heterotrimers: structural mimics of wild-type and mutant collagen type I. *J. Am. Chem. Soc.* 130, 7509–7515.
- (43) Brodsky, B., and Baum, J. (2008) Structural biology: modelling collagen diseases. *Nature* 453, 998–999.
- (44) Fiori, S., Sacca, B., and Moroder, L. (2002) Structural properties of a collagenous heterotrimer that mimics the collagenase cleavage site of collagen type I. *J. Mol. Biol.* 319, 1235–1242.
- (45) Ottl, J., Battistuta, R., Pieper, M., Tschesche, H., Bode, W., Kuhn, K., and Moroder, L. (1996) Design and synthesis of heterotrimeric collagen peptides with a built-in cystine-knot. Models for collagen catabolism by matrix-metalloproteases. *FEBS Lett.* 398, 31–36.
- (46) Kotch, F. W., and Raines, R. T. (2006) Self-assembly of synthetic collagen triple helices. *Proc. Natl. Acad. Sci. U. S. A.* 103, 3028–3033.
- (47) Gauba, V., and Hartgerink, J. D. (2007) Self-assembled heterotrimeric collagen triple helices directed through electrostatic interactions. *J. Am. Chem. Soc.* 129, 2683–2690.
- (48) Dong, H., Paramonov, S. E., and Hartgerink, J. D. (2008) Self-assembly of alpha-helical coiled coil nanofibers. *J. Am. Chem. Soc.* 130, 13691–13695.
- (49) Gauba, V., and Hartgerink, J. D. (2007) Surprisingly high stability of collagen ABC heterotrimer: evaluation of side chain charge pairs. *J. Am. Chem. Soc.* 129, 15034–15041.
- (50) Salem, G., and Traub, W. (1975) Conformational implications of amino acid sequence regularities in collagen. *FEBS Lett.* 51, 94–99.
- (51) Traub, W., and Fietzek, P. P. (1976) Contribution of the alpha<sub>2</sub> chain to the molecular stability of collagen. *FEBS Lett.* 68, 245–249.
- (52) Hulmes, D. J., Miller, A., Parry, D. A., Piez, K. A., and Woodhead-Galloway, J. (1973) Analysis of the primary structure of collagen for the origins of molecular packing. *J. Mol. Biol.* 79, 137–148.
- (53) Venugopal, M. G., Ramshaw, J. A., Braswell, E., Zhu, D., and Brodsky, B. (1994) Electrostatic interactions in collagen-like triple-helical peptides. *Biochemistry* 33, 7948–7956.
- (54) Yang, W., Chan, V. C., Kirkpatrick, A., Ramshaw, J. A., and Brodsky, B. (1997) Gly-Pro-Arg confers stability similar to Gly-Pro-Hyp in the collagen triple-helix of host-guest peptides. *J. Biol. Chem.* 272, 28837–28840.
- (55) Persikov, A. V., Ramshaw, J. A., Kirkpatrick, A., and Brodsky, B. (2005) Electrostatic interactions involving lysine make major contributions to collagen triple-helix stability. *Biochemistry* 44, 1414–1422.
- (56) Xu, F., Zahid, S., Silva, T., and Nanda, V. (2011) Computational design of a collagen A:B:C-type heterotrimer. *J. Am. Chem. Soc.* 133, 15260–15263.
- (57) Fallas, J. A., and Hartgerink, J. D. (2012) Computational design of self-assembling register-specific collagen heterotrimers. *Nat. Commun.* 3, 1087.
- (58) Xu, F., Zhang, L., Koder, R. L., and Nanda, V. (2010) De Novo Self-Assembling Collagen Heterotrimers Using Explicit Positive and Negative Design. *Biochemistry* 49, 2307–2316.
- (59) Savitzky, A. G., and Golay, M. J. E. (1964) Smoothing and differentiation of data by simplified least squares procedures. *Anal. Chem.* 36, 1627.
- (60) Parmar, A. S., and Muschol, M. (2009) Lysozyme as diffusion tracer for measuring aqueous solution viscosity. *J. Colloid Interface Sci.* 339, 243–248.
- (61) Parmar, A. S., Gottschall, P. E., and Muschol, M. (2007) Pre-assembled clusters distort crystal nucleation kinetics in supersaturated lysozyme solutions. *Biophys. Chem.* 129, 224–234.
- (62) Parmar, A. S., and Muschol, M. (2009) Hydration and hydrodynamic interactions of lysozyme: effects of chaotropic versus kosmotropic ions. *Biophys. J.* 97, 590–598.
- (63) Pike, D. H., and Nanda, V. (2015) Empirical Estimation of Local Dielectric Constants: Toward Atomistic Design of Collagen Mimetic Peptides. *Biopolymers* 104, 360.
- (64) Presta, L. G., and Rose, G. D. (1988) Helix signals in proteins. *Science* 240, 1632–1641.
- (65) O'Neil, K. T., and DeGrado, W. F. (1990) A thermodynamic scale for the helix-forming tendencies of the commonly occurring amino acids. *Science* 250, 646–651.
- (66) Hornak, V., Abel, R., Okur, A., Strockbine, B., Roitberg, A., and Simmerling, C. (2006) Comparison of multiple amber force fields and development of improved protein backbone parameters. *Proteins: Struct., Funct., Genet.* 65, 712–725.
- (67) Pang, Y. P., Xu, K., El Yazal, J., and Prendergast, F. G. (2000) Successful molecular dynamics simulation of the zinc-bound farnesyltransferase using the cationic dummy atom approach. *Protein Sci.* 9, 1857–1865.
- (68) Williams, R. J. P., and Frausto da Silva, J. J. R. (1997) *The Natural Selection of the Chemical Elements*, Clarendon Press, Oxford.

- (69) Wray, J. W., Baase, W. A., Ostheimer, G. J., Zhang, X. J., and Matthews, B. W. (2000) Use of a non-rigid region in T4 lysozyme to design an adaptable metal-binding site. *Protein Eng., Des. Sel.* 13, 313–321.
- (70) Nanda, V., Rosenblatt, M. M., Osyczka, A., Kono, H., Getahun, Z., Dutton, P. L., Saven, J. G., and DeGrado, W. F. (2005) De novo design of a redox-active minimal rubredoxin mimic. *J. Am. Chem. Soc.* 127, 5804–5805.
- (71) Kaplan, J., and DeGrado, W. F. (2004) De novo design of catalytic proteins. *Proc. Natl. Acad. Sci. U. S. A.* 101, 11566–11570.
- (72) Zhang, X. J., and Matthews, B. W. (1995) Edpdbl - a Multifunctional Tool for Protein-Structure Analysis. *J. Appl. Crystallogr.* 28, 624–630.
- (73) Fleishman, S. J., and Baker, D. (2012) Role of the biomolecular energy gap in protein design, structure, and evolution. *Cell* 149, 262–273.
- (74) Havranek, J. J., and Harbury, P. B. (2003) Automated design of specificity in molecular recognition. *Nat. Struct. Biol.* 10, 45–52.
- (75) Frank, S., Kammerer, R. A., Mechling, D., Schulthess, T., Landwehr, R., Bann, J., Guo, Y., Lustig, A., Bachinger, H. P., and Engel, J. (2001) Stabilization of short collagen-like triple helices by protein engineering. *J. Mol. Biol.* 308, 1081–1089.
- (76) Stetefeld, J., Frank, S., Jenny, M., Schulthess, T., Kammerer, R. A., Boudko, S., Landwehr, R., Okuyama, K., and Engel, J. (2003) Collagen stabilization at atomic level: crystal structure of designed (GlyProPro)10foldon. *Structure* 11, 339–346.
- (77) Yoshizumi, A., Fletcher, J. M., Yu, Z., Persikov, A. V., Bartlett, G. J., Boyle, A. L., Vincent, T. L., Woolfson, D. N., and Brodsky, B. (2011) Designed coiled coils promote folding of a recombinant bacterial collagen. *J. Biol. Chem.* 286, 17512–17520.
- (78) Xu, Y., Keene, D. R., Bujnicki, J. M., Hook, M., and Lukomski, S. (2002) Streptococcal Scl1 and Scl2 proteins form collagen-like triple helices. *J. Biol. Chem.* 277, 27312–27318.
- (79) Yu, Z., Mirochnitchenko, O., Xu, C., Yoshizumi, A., Brodsky, B., and Inouye, M. (2010) Noncollagenous region of the streptococcal collagen-like protein is a trimerization domain that supports refolding of adjacent homologous and heterologous collagenous domains. *Protein Sci.* 19, 775–785.
- (80) Pires, M. M., Przybyla, D. E., Rubert Perez, C. M., and Chmielewski, J. (2011) Metal-mediated tandem coassembly of collagen peptides into banded microstructures. *J. Am. Chem. Soc.* 133, 14469–14471.
- (81) Moriarty, G. M., Minetti, C. A., Remeta, D. P., and Baum, J. (2014) A revised picture of the Cu(II)-alpha-synuclein complex: the role of N-terminal acetylation. *Biochemistry* 53, 2815–2817.
- (82) (1957) *Stability Constants of Metal-Ion Complexes, with Solubility Products of Inorganic Substances*, Special Publications, No. 6, The Chemical Society, London.
- (83) Dahl, S. L. M., Rucker, R. B., and Niklason, L. E. (2005) Effects of copper and cross-linking on the extracellular matrix of tissue-engineered arteries. *Cell Transplant* 14, 367–374.